

COMPARATIVE ANALYSIS OF A NOVEL LOW CONCENTRATION DUAL PHOTOVOLTAIC/PHASE CHANGE MATERIAL SYSTEM WITH A NON-CONCENTRATOR PHOTOVOLTAIC SYSTEM

by

Jawad SARWAR^{a*}, Arshmah HASNAIN^a, Ahmed E. ABBAS^b, and Konstantinos E. KAKOSIMOS^b

^a Department of Mechanical Engineering,
University of Engineering and Technology, Lahore, Pakistan

^b Sustainable Energy and Clean Air Research Laboratory,
Texas A&M University at Qatar, Doha, Qatar

Original scientific paper
<https://doi.org/10.2298/TSCI190929468S>

In this work, a novel design of a concentrated photovoltaic system with thermal management using phase change material is analyzed. The novelty lies in utilizing two mono-facial photovoltaic cells, installing one on upper side of the receiver to receive non-concentrated sunlight and installing another photovoltaic cell on bottom side to receive concentrated sunlight. An RT47 (melting range of 41-48 °C) phase change material enclosed in an aluminum containment regulates the temperature of the system. Parabolic trough concentrator is used to focus sunlight on the bottom photovoltaic cell with a concentration ratio of 25. A finite volume based coupled thermal, electrical and optical model is developed and the system is analyzed for environmental conditions of Doha, Qatar. Temperature regulation and electrical power output of upper photovoltaic cell and bottom concentrated photovoltaic cell of proposed design are compared to a conventional flat plate system. Analysis is made for one day of each month of a year. It is found that the proposed design maintains the temperature below 85 °C for all months of a year. The performance of the proposed system is comparable to the conventional flat plate system and excels it with power production in the range of -4.7% and +21.7%.

Key words: *concentrated photovoltaic, phase change material, finite element method*

Introduction

Solar energy-based technologies have a huge potential in clean renewable energy resources due to consistent and abundant supply [1]. One common application of solar technologies is concentrated photovoltaics (CPV) system that converts solar irradiance directly to electricity. However, concentrating sunlight can significantly increase the temperature of a CPV system. The efficiency of crystalline silicon PV cell decreases with the increase in the PV's temperature by an average of 0.0045 °C⁻¹ [2]. Phase change materials (PCM) have been employed to regulate the temperature of the PV [3]. The PCM absorbs the excess heat generated as latent heat of fusion at constant phase transition temperature and maintains the operating temperature of the PV. The time and the temperature range of the melting/solidification process of the PCM depend on the mass and thermal conductivity of PCM [4].

* Corresponding author, e-mail: jawad.sarwar@uet.edu.pk

The performance of PV modules is dependent on their orientation as studied experimentally by Pantic *et al.* [5]. Several researchers have investigated, theoretically and experimentally, the thermal and electrical performance of CPV using PCM (CPVPCM) and are tabulated in tab. 1. It is reported that a PCM is effective in temperature reduction of CPVPCM system. It reduces cost per unit power output of the system and increases CPVPCM system's electrical and thermal efficiency [6-12].

Table 1. Experimental and theoretical investigations

Type of investigations	Concentration ratio	References
Experimental	4	[11]
Theoretical	5, 10, and 20	[6]
Experimental	2.8	[10]
Experimental and theoretical	1.3	[8]
Experimental	<3	[12]
Theoretical	3, 5, 8, and 10	[9]
Experimental and theoretical	2	[7]
Experimental	1-7	[13]
Experimental	1-12	[14]
Experimental	1-6	[15]

Bifacial PV cells have also been employed in CPV systems due to their ability to increase power production as compared to the best efficiency mono-facial cell [16]. An extensive review on bifacial cell technology is presented in [17]. A flat plate static concentrator design was presented by [18] which comprised of 24 mm wide bifacial PV cell and 12 mm wide V-grooved reflector sheet, placed side by side and a cover glass of thickness 3.2 mm. The bifacial cell is placed higher than the reflector sheet level to make it accept light at the rear surface as well. Mono-facial and bifacial cells of concentration ratio (CR) 1.5 and 2, respectively, were analyzed. It is reported that the flat plate static concentrator with bifacial PV cell increased power production by 2% as compared to mono-facial PV cell [18]. Two design variants of low parabolic trough concentration PV system employing bifacial PV cells were presented by Poulek *et al.* [19]. In the first variant, PV module was placed horizontally and parallel to the tracking axis and the geometric CR was 3.6. In the second variant, the module was placed vertically, and the geometric CR was 4.1. The maximum daily energy gain was 167% and 114% as compared to the conventional fixed PV module for first and second variants, respectively. Further studies conducted to evaluate the performance of bifacial cells under concentrated irradiance are tabulated in tab. 1 [13-15]

Although, CPV system with bifacial cells produce more electrical power as compared to similar CPV system with mono-facial cells but no thermal management technique can be used by such systems. In the absence of a thermal management system, the bifacial cell temperature increases beyond 90 °C [19] at CR of 3.6 or higher. This problem restricts bifacial cells application and it cannot be used for medium concentration ($CR \geq 10$) or high concentration ($CR \geq 100$). In this work, a novel configuration of a CPV system integrated with a PCM is proposed. This configuration uses two mono-facial PV cells instead of bifacial PV cells and temperature is controlled using PCM. The thermal and electrical output is compared with a conventional flat-plate PV system to assess its effectiveness.

Materials and methods

Physical model

Schematic illustration of the CPV system integrated with a PCM is considered in this work as shown in fig. 1. The system consists of a non-ideal parabolic trough concentrator with single-axis tracking and a receiver. The receiver employs two mono-facial crystalline Si PV cells (upper and bottom) and a PCM to passively regulate the temperature of both PV cells. The system is referred to dCPVPCM system in the subsequent text. The concentrator focuses sunlight on a 15 mm wide bottom PV cell. The bottom PV cell is attached to an aluminum container which encapsulates the PCM. A 100 mm wide upper PV cell is also attached to the aluminum container which is concomitantly exposed to non-concentrated sunlight. The PV cell is covered with layers of ethylene vinyl acetate, anti-reflective coating, and tedler with an additional layer of glass for the upper PV having dimensions as shown in fig. 1. The RT47 is selected as a PCM that has a phase transition temperature of 41-48 °C. The CR of 25 is considered for dCPVPCM system having a length of 2.13 m which results in a 1 m² footprint. The system is analyzed for optical, thermal and electrical behavior. The results are compared with a conventional PV system having an inclination angle of -25.3° with true South orientation. Both systems are simulated for environmental conditions of Doha, Qatar (latitude and longitude of 25.314779° N and 51.43978° E, respectively).

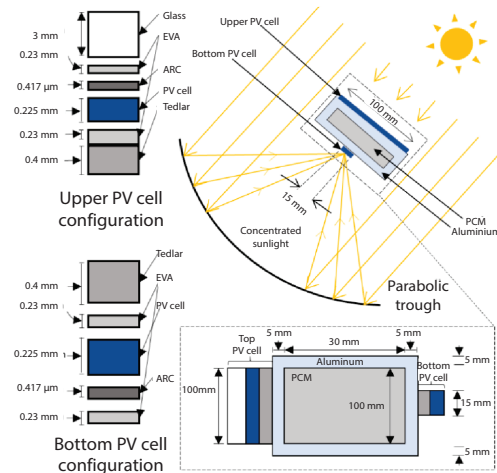


Figure 1. Schematic illustration of the CPV system integrated with PCM (not to scale)

The dCPVPCM system is subjected to direct beam irradiance while PV system is subjected to global horizontal irradiance. Input values of irradiance for both systems are attained by clear sky broadband solar radiation model [20]. The weather data comprises ambient temperature and wind speed for the selected days. Weather data is obtained from experimentally determined data by the Meteorological Department, Qatar. The mean maximum temperature for the period of 1962-2013 is reported to be 41.9 °C for the month of July [21]. The proposed design is analyzed for maximum temperature of 45 °C in month of July to ensure that the very hot days are included in the analysis. The variations of the input parameters with time are shown in fig. 2.

Theoretical model

The five parameters model is used to analyze the electrical behaviour of dCPVPCM and PV systems. The parameters include photocurrent, I_{PV} , reverse saturation diode current, I_o , shunt and series resistances, R_p and R_s , and diode ideality or quality factor, a . The following equation relates the five mentioned parameters with current and voltage:

$$I = I_{PV} - I_o \left(\exp \frac{V + R_s I}{V_i a} \right) - \frac{V + R_s I}{R_p} \quad (1)$$

where V_i is the thermal voltage of the array. The algorithm is derived from Villalva *et al.* [22] and modified for varying temperature and irradiance. It uses an iterative process to find the values

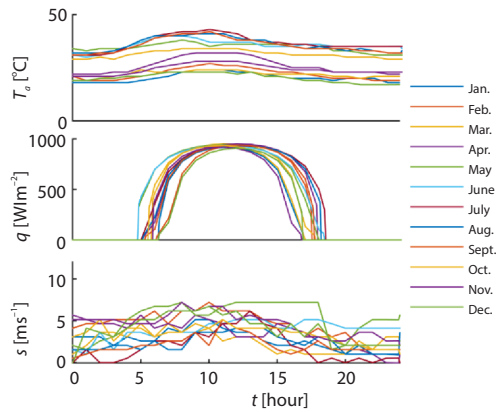


Figure 2. Ambient temperature, irradiance, and wind speed data

of R_p and R_s for which the maximum error ε_{tol} in the values of calculated maximum power $P_{\text{max,m}}$ and experimental maximum power $P_{\text{max,e}}$ is 0.0001 (arbitrarily chosen). Model provides results precisely for standard conditions of 25 °C temperature and 1000 W/m² irradiance. To predict the electrical behavior at different temperatures and irradiances, values of I_{PV} and I_o are corrected. The I_{PV} is assumed to be linearly related to irradiance and I_o as function of temperature with R_p and α being constant. Short circuit current I_{sc} being function of temperature and irradiance, and open circuit voltage V_{oc} being function of temperature are modified with help of temperature coefficients, K_I and K_V , as:

$$I_{\text{sc}} = \frac{(I_{\text{sc},n} + K_I \Delta T) \mathbf{q}}{G_n} \quad (2)$$

$$V_{\text{oc}} = (V_{\text{oc},n} + K_V \Delta T) \quad (3)$$

where ΔT is the temperature difference relative to standard value and G_n is the nominal irradiance. The corrected values of I_{PV} and I_o are calculated using the modified values of I_{sc} and V_{oc} . Since R_s decreases with irradiance its value is modified using relation $R_s = R_{s,n}(G_n/G)$ [23]. The IV curves are generated using Newton-Raphson iterative method.

In this work, a finite volume thermal model is developed using 2-D differential heat diffusion equation. Convection and radiation effects are considered at the boundary only. To achieve transformation of physical co-ordinates to natural co-ordinates, an 8-node Serendipity element is used as shape function. Detailed thermal optical model is presented by authors' elsewhere [24] but transformed energy balance equation in terms of mass, \mathbf{M} , conductivity, \mathbf{K} , irradiance, \mathbf{q} , convection, \mathbf{H} , and radiation, \mathbf{R} , matrices is presented in eq. (4):

$$\mathbf{M}\dot{T} + \mathbf{K}T - \mathbf{q} + (\mathbf{H} + \mathbf{R})T = 0 \quad (4)$$

where T is the temperature and \dot{T} – the time derivative. The optical model accounts for the reflection and the absorption losses at both, CPV and PV covers and is calculated using Fresnel equations. The incident irradiance, q_i , is updated after the optical losses through the layers on PV and depending on the electrical conversion efficiency of the PV cell. This requires a combined electrical and optical losses effect in irradiance which is incorporated using the following equations:

$$q_{\text{aol}} = (1 - \rho - \alpha) q_i, \quad q_e = [\eta_{\text{ei-STC}} + \mu(T - T_a)] q_{\text{aol}}, \quad q = q_{\text{aol}} - q_e \quad (5)$$

where q_{aol} is the available irradiance after optical losses of absorption α and reflection ρ , q_e – the part of irradiance that is converted to electricity depending on the electrical efficiency $\eta_{\text{ei-STC}}$ and temperature coefficient of power output μ measured at standard test conditions. Crank-Nicholson method is used for temporal discretization. Both systems are solved at each time step with updated convection, radiation and electrical conversion of irradiance. Timestep of 300 seconds

and 24600 elements with 75081 nodes are selected for the current study after performing grid-time independence studies. Total thermal energy, Q_s , stored in PCM is calculated by eq. (6) as per the temperature conditions. Thermal and overall efficiencies are calculated using eqs. (7) and (8). The mathematical model is validated by the authors' elsewhere [24]. The relevant properties of the materials are presented in tab. 2.

$$Q_s = \begin{cases} mc_s(T - T_1) & T < T_1 \\ mc_s(T_1 - T) + mc_e(T - T_1) & T_1 \leq T \leq T_2 \\ mc_s(T_1 - T) + mc_e(T - T_1) + mc_l(T - T_2) & T > T_2 \end{cases} \quad (6)$$

$$\eta_{th} = \frac{\sum Q_s}{\int q(t) A dt} \quad (7)$$

$$\eta = \eta_{th} + \eta_{el} \quad (8)$$

Table 2. Relevant properties of the materials

Thermal properties					
Material	T_m [°C]	H [kJkg ⁻¹]	K [Vm ⁻¹ K ⁻¹]	ρ [kgm ⁻³]	C_o [kJkg ⁻¹ K ⁻¹]
RT47	41-48	165	0.2	880	2 (solid, liquid)
Aluminum	–	–	211	2675	0.9
PV cell	–	–	125.4	2205	0.8
Electrical Properties					
I_{sc} [A]	V_{oc} [V]	I_{mp} [A]	V_{pm} [V]	K_I [%K ⁻¹]	K_V [%K ⁻¹]
8.21	32.9	7.61	26.3	0.0032	-0.1
Optical Properties					
	Refractive index	Extinction coefficient [m ⁻¹]	Depth (m)		
PV	4	4710	5 · 10 ⁻⁴		

Validation

The temperature output of a PV and PVPCM systems reported in [25] is used to compare the temperature output of the developed model. Both systems employ a polycrystalline PV panel with a rated capacity of 40 W and conversion efficiency of 15%. A paraffin wax, RT42 is used as a PCM. The PCM is encapsulated in an aluminum container and attached to the back of the PV. Both, PV and PVPCM systems were tested for a year under outdoor conditions at the latitude and longitude of 24.1° N and 55.8° E, respectively. The details of the geometrical dimensions of the system and thermophysical properties of the materials can be found elsewhere [25]. Both systems are simulated using developed model and employing reported geometrical configuration and thermophysical properties of the used materials. The temperature output of the experimental results is compared with the temperature output of the simulated results. The comparison of temperature of PV in a PVPCM system is shown in fig. 3(a) while the comparison of PV temperature in a PV system is shown in fig. 3(b). The result has shown a good agreement between experimental and simulated results with an average standard deviation of < ±3% which is comparable to the reported cumulative experimental uncertainty of 5.26%.

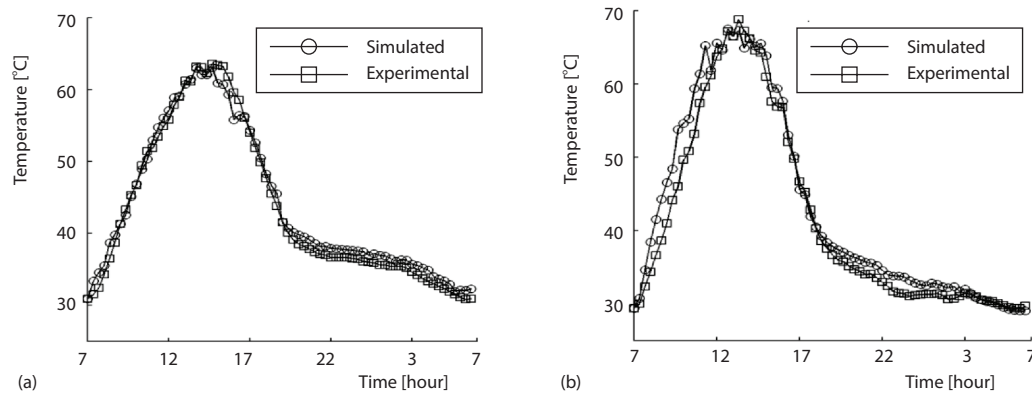


Figure 3. Validation of thermal output of the model; (a) comparison of temperature of PV in a PVPCM system and (b) comparison of PV temperature in a PV system

Results and discussion

Temperature for one day of each month was determined for the upper PV and bottom CPV cell of the dCPVPCM system and it is compared with flat-plate PV system, referred to PV only in subsequent text. The comparison of temperature results for one day of all the months is shown in fig. 4. It is found that the operating temperature of the CPV cell and the upper PV cell stay below $85\text{ }^{\circ}\text{C}$ during all months in a year. The peak CPV cell temperature is comparable to the PV only temperature with a maximum variation of $\pm 4\text{ }^{\circ}\text{C}$ except for the month of March when

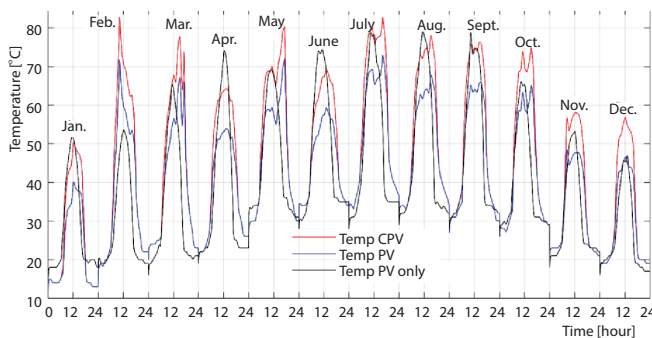


Figure 4. Temperature results for upper PV, bottom CPV, and conventional PV system

maximum temperature is $+12.3\text{ }^{\circ}\text{C}$ higher than the PV only temperature. A peak shifting in temperature is observed for dCPVPCM system *i. e.* the peak temperature for dCPVPCM system is found after ~ 1 hour the peak temperature of the PV only. This peak shifting is due to the inclusion of PCM in the dCPVPCM system and this behavior is consistent with the previously reported results for non-CPV systems integrated with phase change materials [4].

Further analysis is carried out to find maximum, and average temperature of the dCPVPCM system and PV only and result is shown in fig. 5.

It is found that the average temperature of CPV cell and upper PV cell consistently stays below or almost equal to the average temperature of PV only for the months of January and September as shown in fig. 5. On the other hand, the maximum temperature of CPV cell consistently stays higher or almost equal to the maximum temperature of PV only. It is also found that the CPV cell operates at a higher average and maximum temperature as compared to the upper PV. To analyze this behavior, temperature contours are plotted at different times of a day *i. e.* 10 a. m., 1 p. m., and 4 p. m., and result is shown in fig. 6. It is found that the temperature evolves from the bottom CPV cell with a higher temperature towards the upper PV cell. Al-

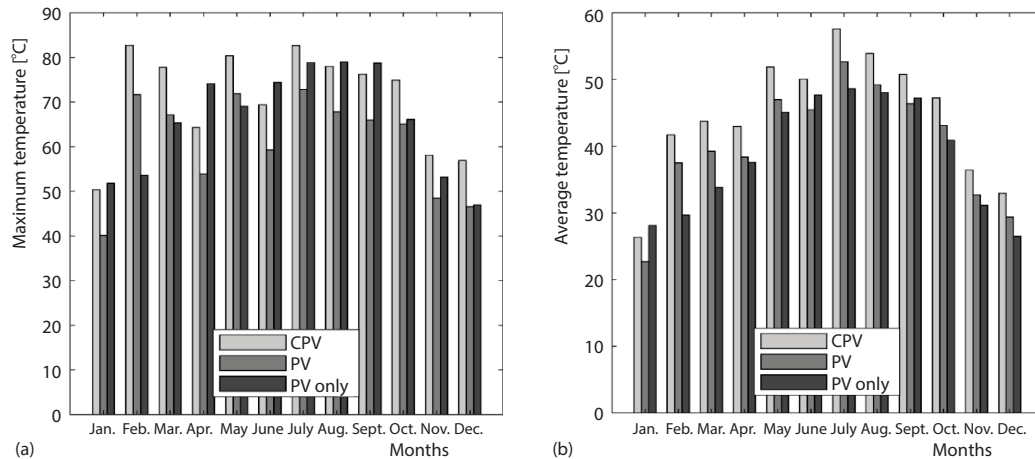


Figure 5. (a) Maximum cell temperatures for PV and CPV cells of dCPVPCM vs. PV only and (b) average cell temperatures for PV and CPV cells of dCPVPCM vs. PV only

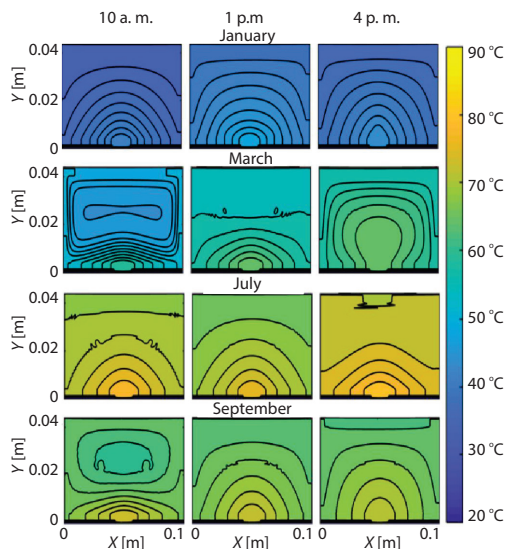


Figure 6. Temperature contours for the domain of dCPV/PCM system

though, dCPVPCM receives irradiance for both bottom CPV cell and upper PV cell but the heat flow from the bottom CPV cell towards the upper PV cell shows that the concentrated irradiance plays dominant role in generating heat in the current configuration. That is why the CPV cell operates at a higher temperature as compared to the upper PV cell as shown in figs. 4 and 5. Temperature contours in fig. 6 also show that the temperature conducts faster at the sides of dCPVPCM system (aluminum containment) as compared to in the center (PCM) of the dCPVPCM system. This behavior is due to the different conductivities of the materials. The aluminum containment conducts fast due to its higher conductivity (211 W/mK) as compared to the PCM which has a lower conductivity (0.2 W/mK). Due to the higher conductivity of the aluminum, the PCM is also heated from the sides as shown by temperature contours in the

PCM. The thermal analysis of dCPVPCM system shows that the current configuration controls the temperature of both CPV and PV cells and maintain their temperature below 85 °C which is essential for the durability of crystalline Si PV cell.

Further analysis is carried out to obtain the power produced by individual cells of dCPVPCM and PV only and the result is presented in fig. 7 while the combined power obtained by both cells of dCPVPCM and PV only is presented in fig. 8. Although, the maximum power from individual cells of dCPVPCM is smaller than PV only, the average power of individual CPV cell is comparable to that of PV only cell. The combined average power of dCPVPCM is nearly equal to that of PV only and exceeds the power obtained from PV only with a maximum difference of +21.8% for January. This behavior is consistent with the temperature be-

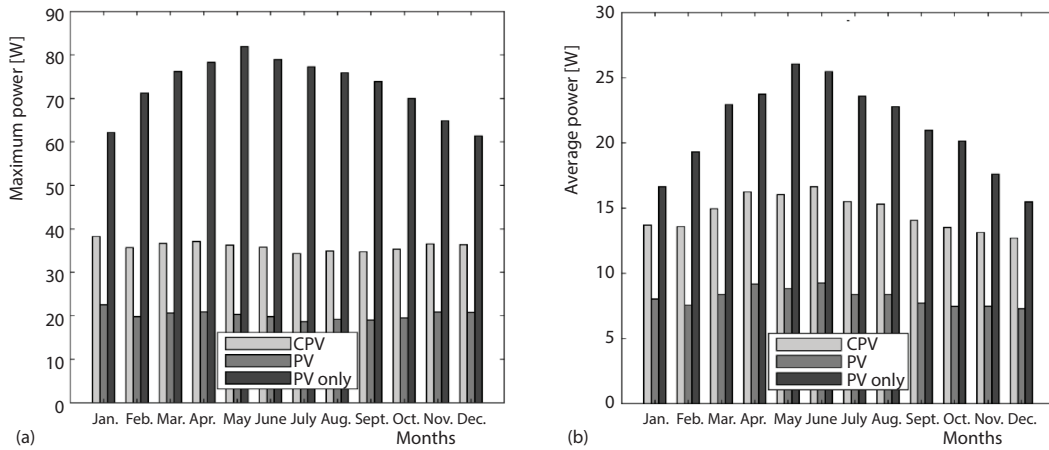


Figure 7. Maximum cell power for PV and CPV cells of dCPVPCM vs. PV only and (b) average cell power for PV and CPV cells of dCPVPCM vs. PV only

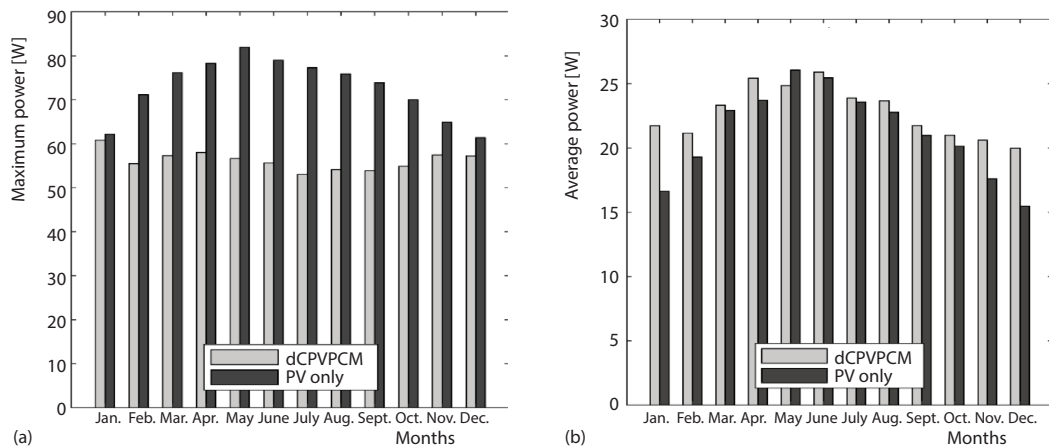


Figure 8. Combined maximum cell power for both cells of dCPVPCM vs. PV only and (b) combined average cell power for both cells of dCPVPCM vs. PV only

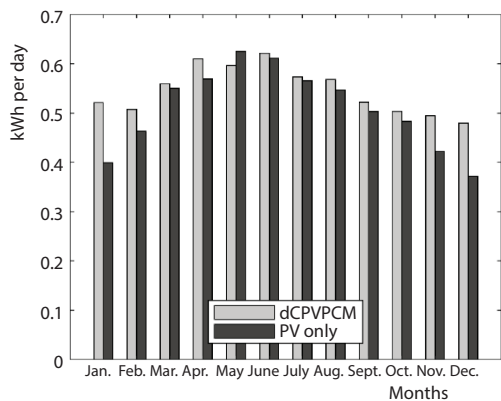


Figure 9. Combined kWh per day available from both cells of dCPVPCM vs. PV only

havior for January, refer to fig. 5, as the average temperature of both CPV and PV cell remains below the PV only temperature which results in increased power production. The average power of dCPVPCM is only less than that of PV only for the month of May with a difference of 4.7%. The maximum power falls for the months of summer due to greater temperature rise but the average power of dCPVPCM remains consistently higher than that of PV only. This is due to the utilization of dual sides for power production and shows that proposed design can produce electrical power higher than PV only over the year.

To further investigate and compare the power production by dCPVPCM system and PV only, the power produced over the day is calculated and result is shown in fig. 9. The dCPVPCM system produces power in the range of -4.7% to $+21.7\%$ as compared to PV only system.

Conclusion

Proposed design of dCPVPCM is found to be effective for temperature regulation of cells below $85\text{ }^{\circ}\text{C}$. The combined power obtained from proposed dCPVPCM design is comparable to that obtained from a conventional flat plate system and excels with power production in the range of -4.7 to $+21.7\%$. Therefore, it can be concluded that the proposed dCPVPCM system is useful to generate electricity and performs better or comparable than the conventional PV only system in terms of electrical output. The proposed dCPVPCM system also replaces expensive crystalline Si material with an inexpensive concentrator material with an added advantage of storing thermal energy in the PCM, therefore, it can be considered better than the PV only system. Further studies are required to investigate cost analysis of the proposed system as well as optimization of the dCPVPCM system in terms of geometry and materials.

Acknowledgment

This publication was made possible by a PDRA award [PDRA2-1105-14044] from the Qatar National Research Fund (a member of The Qatar Foundation). The statements made herein are solely the responsibility of the authors. The HPC resources and services used in this work were provided by the IT Research Computing group in Texas A&M University at Qatar. IT Research Computing is funded by the Qatar Foundation for Education, Science and Community Development (<http://www.qf.org.qa>). The authors would also like to acknowledge the department of mechanical engineering, University of Engineering and Technology, Lahore for their invaluable support in conducting this research work.

Nomenclature

a – diode ideality or quality factor
 G – irradiance, [Wm^{-2}]
 G_n – normal irradiance, [Wm^{-2}]
 \mathbf{H} – convection matrix
 I_{PV} – photocurrent, [A]
 I_{sc} – short circuit current, [A]
 I_o – reverse saturation diode current, [A]
 \mathbf{K} – conductivity matrix
 K_I – temperature coefficients of current
 K_V – temperature coefficients of voltage
 \mathbf{M} – mass matrix
 $P_{max,e}$ – experimental maximum power, [W]
 $P_{max,m}$ – calculated maximum power, [W]
 Q_s – total thermal energy, [W]
 \mathbf{q} – irradiance matrix
 q_{aol} – available irradiance after optical losses, [Wm^{-2}]
 q_e – part of irradiance converted to electricity, [Wm^{-2}]
 q_i – incident irradiance, [Wm^{-2}]
 \mathbf{R} – radiation matrix

R_p – shunt resistances
 R_s – series resistances
 T – temperature, [K]
 V – output voltage
 V_{oc} – open circuit voltage, [V]
 V_t – thermal voltage, [V]

Greek letters

α – absorption
 ϵ_{tol} – maximum error
 η_{ei-STC} – electrical efficiency at standard conditions
 μ – temperature coefficient of power output
 ρ – reflection

Acronyms

CPV – concentrated photovoltaic
 CR – concentration ratio
 dCPVPCM – dual concentrated photovoltaic with phase change material
 PV – photovoltaic
 PCM – phase change material

References

- [1] Browne, M. C., *et al.*, Assessing the Thermal Performance of Phase Change Material in a Photovoltaic/Thermal System, *Energy Procedia*, 91 (2016), June, pp. 113-121

- [2] Skoplaki, E., Palyvos, J. A., On the Temperature Dependence of Photovoltaic Module Electrical Performance: A Review of Efficiency/Power Correlations, *Solar Energy*, 83 (2009), 5, pp. 614-624
- [3] Huang, M. J., et al., Thermal Regulation of Building-Integrated Photovoltaics Using Phase Change Materials, *International Journal of Heat and Mass Transfer*, 47 (2004), 12, pp. 2715-2733
- [4] Browne, M. C., et al., Phase Change Materials for Photovoltaic Thermal Management, *Renewable and Sustainable Energy Reviews*, 47 (2015), July, pp. 762-782
- [5] Pantic, L.S., et al., Electrical Energy Generation with Differently Oriented Photovoltaic Modules as Façade Elements, *Thermal Science*, 20 (2016), 4, pp. 1377-1386
- [6] Emam, M., et al., Performance Enhancement of Concentrated Photovoltaic System Using Phase-Change Material, *Proceedings*, 10th, Int. Conf. on Energy Sustainability, Charlotte, N. C., USA, 2016, Vol. V001T08A006
- [7] Lu, W., et al., Investigation on Designed Fins-Enhanced Phase Change Materials System for Thermal Management of a Novel Building Integrated Concentrating PV, *Applied Energy*, 225 (2018), Sept., pp. 696-709
- [8] Maiti, S., et al., Self Regulation of Photovoltaic Module Temperature in V-trough Using a Metal-Wax Composite Phase Change Matrix, *Solar Energy*, 85 (2011), 9, pp. 1805-1816
- [9] Manikandan, S., et al., Thermal Management of Low Concentrated Photovoltaic Module with Phase Change Material, *Journal of Cleaner Production*, 219 (2019), May, pp. 359-367
- [10] Sarmah, N., et al., Design, Development and Indoor Performance Analysis of a Low Concentrating Dielectric Photovoltaic Module, *Solar Energy*, 103 (2014), May, pp. 390-401
- [11] Sarwar, J., et al., Experimental Investigation of Temperature Regulation of Concentrated Photovoltaic Using Heat Spreading and Phase Change Material Cooling Method, *Proceedings*, 2nd Int. Conf. on Sustainable Energy Storage, Dublin, Ireland, 2013
- [12] Tabet Aoul, K., et al., Energy Performance Comparison of Concentrated Photovoltaic – Phase Change Material Thermal (CPV-PCM/T) System with Flat Plate Collector (FPC), *Solar Energy*, 176 (2018), Dec., pp. 453-464
- [13] Untila, G. G., et al., Fluorine- and Tin-Doped Indium Oxide Films Grown by Ultrasonic Spray Pyrolysis: Characterization and Application in Bifacial Silicon Concentrator Solar Cells, *Solar Energy*, 159 (2018), Jan., pp. 173-185
- [14] Untila, G. G., et al., Concentrator In₂O₃:F/(n+pp+)c-Si/Al Solar Cells with Al-Alloyed BSF and Ag-Free Multi-Wire Metallization Using Transparent Conductive Polymers, *Solar Energy*, 174 (2018), Nov., pp. 1008-1015
- [15] Untila, G., et al., Bifacial IFO/(n+ pp+) Cz-Si/ITO Solar Cells with Full-Area Al-Alloyed BSF and Ag-Free Multi-Wire Metallization Suitable for Low-Concentration Systems, *Solar Energy*, 193 (2019), Nov., pp. 992-1001
- [16] Sun, Y., et al., Tailoring Interdigitated Back Contacts for High-Performance Bifacial Silicon Solar Cells, *Applied Physics Letters*, 114 (2019), 10, 103901
- [17] Guerrero-Lemus, R., et al., Bifacial Solar Photovoltaics – A Technology Review, *Renewable and Sustainable Energy Reviews*, 60 (2016), July, pp. 1533-1549
- [18] Uematsu, T., et al., Fabrication and Characterization of a Flat-Plate Static-Concentrator Photovoltaic Module, *Solar Energy Materials and Solar Cells*, 67 (2001), 1, pp. 425-434
- [19] Poulek, V., et al., Innovative Low Concentration PV Systems with Bifacial Solar Panels, *Solar Energy*, 120 (2015), Oct., pp. 113-116
- [20] Bird, R. E., Hulstrom, R. L., Simplified Clear Sky Model for Direct and Diffuse Insolation on Horizontal Surfaces, Report, Solar Energy Research Inst., Golden, Co., USA, 1981
- [21] ***, <https://qweather.gov.qa/CAA/ClimateNormals.aspx>.
- [22] Villalva, M. G., et al., Comprehensive Approach to Modelling and Simulation of Photovoltaic Arrays, *IEEE Transactions on Power Electronics*, 24 (2009), 5, pp. 1198-1208
- [23] Lo Brano, V., et al., An Improved Five-Parameter Model for Photovoltaic Modules, *Solar Energy Materials and Solar Cells*, 94 (2010), 8, pp. 1358-1370
- [24] Sarwar, J., et al., Effect of the Phase Change Material's Melting Point on the Thermal Behaviour of a Concentrated Photovoltaic System in a Tropical Dry Climate, *Proceedings*, ISES Conference Proceedings, Palma de Mallorca, Spain, 2016
- [25] Hasan, A., et al., Yearly Energy Performance of a Photovoltaic-Phase Change Material (PV-PCM) System in Hot Climate, *Solar Energy*, 146 (2017), Apr., pp. 417-429